Molecular Distributions in Interphases: Statistical Mechanical Theory Combined with Molecular Dynamics Simulation of a Model Lipid Bilayer

Tian-xiang Xiang and Bradley D. Anderson
Department of Pharmaceutics and Pharmaceutical Chemistry, University of Utah, Salt Lake City, Utah, USA

ABSTRACT A mean-field statistical mechanical theory has been developed to describe molecular distributions in interphases. The excluded volume interaction has been modeled in terms of a reversible work that is required to create a cavity of the solute size against a pressure tensor exerted by the surrounding interphase molecules. The free energy change associated with this compression process includes the configurational entropy as well as the change in conformational energy of the surrounding chain molecules. The lateral pressure profile in a model lipid bilayer (30.5 Å^2/chain molecule) has been calculated as a function of depth in the bilayer interior by molecular dynamics simulation. The lateral pressure has a plateau value of 309 ± 48 bar in the highly ordered region and decreases abruptly in the center of the bilayer. Model calculations have shown that for solute molecules with ellipsoidal symmetry, the orientational order increases with the ratio of the long to short molecular axes at a given solute volume and increases with solute volume at a given axial ratio, in accordance with recent experimental data. Increased lateral pressure ($p_\perp$) results in higher local order and exclusion of solute from the interphase, in parallel with the effect of surface density on the partitioning and local order. The logarithm of the interphase/water partition coefficient for spherical solutes decreases linearly with solute volume. This is also an excellent approximation for elongated solutes because of the relatively weak dependence of solute partitioning on molecular shape. The slope is equal to $(2p_\perp - p_\parallel)/3k_BT$, where $p_\parallel$ is the normal pressure component, and different from that predicted by the mean-field lattice theory. Finally, the lattice theory has been extended herein to incorporate an additional constraint on chain packing in the interphase and to account for the effect of solute size on partitioning.

INTRODUCTION

The properties of the interfacial region separating two bulk phases may differ substantially from those of the bulk phases themselves. Common to many of these interfacial regions are domains, termed "interphases" (Dill and Flory, 1980; Naghizadeh and Dill, 1991), which can be modeled as an ensemble of hydrophobic chain molecules having one end restrained or anchored to a surface. Interphase properties govern a multitude of processes involving biological membranes; surfactant films; micelles and other amphiphilic aggregates, adhesives, lubricants; and the stationary phases used in reversed-phase liquid chromatography. Solute distributions in interphases have particular importance. For example, the therapeutic potency and toxicity of drug molecules (e.g., anesthetics) are closely related to their partition coefficients between an aqueous solution and the interior of a biological membrane (Davis et al., 1974). Retention volumes in reversed-phase liquid chromatography are proportional to the partition coefficients of analytes between the mobile phase and the stationary phase, which consists of alkyl chains grafted onto silica surfaces (Dill, 1987).

Constraints imposed by interfacial forces result in partial chain ordering and a variation in molecular organization with depth from the surface in interphases (Dill and Flory, 1981; Seelig and Seelig, 1974). Solute partitioning into interphases is closely related to this local chain ordering and anisotropy, and differs from partitioning into bulk fluid phases in several important respects. First, the distribution of solute within an interphase is not uniform, reflecting the variation in local chain order. Solute concentrations are highest in the more disordered regions which, in bilayers, are in the vicinity of the bilayer midplane (White et al., 1981). Second, relative to bulk fluid phases of the same chemical character, solute partitioning into interphases is less favorable (Dill et al., 1988) and highly selective to solute size and shape, as evident in the high resolution attainable in chromatographic separations on the basis of size and shape differences (Wise et al., 1981). Similarly, permeabilities in lipid bilayer membranes exhibit an unusually high selectivity of the membrane to permeant size (Lieb and Stein, 1986; Xiang and Anderson, submitted for publication) consistent with recent observations in this laboratory that the barrier domain in lecithin/decane bilayers resides in the highly ordered hydrocarbon chain region (Xiang and Anderson, submitted for publication; Xiang et al., 1992). Finally, partition coefficients decrease significantly with increasing surface density, as demonstrated in both lipid bilayer partitioning studies (DeYoung and Dill, 1988, 1990) and in reversed-phase chromatography (Wise and May, 1983). Selectivity to solute size and shape increases with increasing surface density in reversed-phase liquid chromatography (Wise and May, 1983).

Several statistical mechanical theories based on lattice models or a unified model of a variational theory have been developed to describe the distributions of molecules in interphases (Ben-Shaul et al., 1984; Viovy et al., 1987; Dill and Flory, 1981; Scheutjens and Fleer, 1979; Theodorou, 1988).

Received for publication 4 October 1993 and in final form 23 December 1993.

Address reprint requests to Dr. Tian-xiang Xiang, Department of Pharmaceutics and Pharmaceutical Chemistry, The University of Utah, 421 Wakara Way, Suite 315, Salt Lake City, UT 84108.

0006-3495/94/03/561/13 $2.00

In the theory of Marqusee and Dill (1986), the interphase interior is represented by a cubic lattice with each chain molecule occupying contiguous sites on the lattice. The chain configurational entropy is calculated subject to packing constraints which arise from the requirement that all lattice sites be occupied. Lattice theory predicts gradients of solute concentration at equilibrium due to the variation of chain organization with depth. However, the simplified representation of chain molecules in the lattice models and the fact that the packing constraints imposed may not be complete may limit the utility of mean-field lattice theory for predicting molecular distributions in real interphases.

A statistical mechanical theory based on the concept of free volume has been proposed for the steric partition behavior of molecules in both random and ordered membrane structures (Giddings et al., 1968; Ogston, 1958; Schnitzer, 1988), but solutions can be obtained only for certain geometries (e.g., a uniform meshwork of cylindrical fibers). For a partially ordered interphase, the free volume does not have a uniform geometry or orientation profile, nor is it exponentially distributed (Xiang, 1993). Thus it is not reasonable to assume a priori that the partition coefficient for a solute of finite size should be either linearly or exponentially dependent on solute volume.

In spite of progress on both the experimental and theoretical fronts, a simple yet predictive general theory is still lacking that is capable of describing molecular distributions, including orientational and conformational distributions in real interphases, and is applicable to a wide range of solute molecules once the interphase thermodynamic state is characterized by a few well-defined physical quantities. In particular, detailed theories that can account for the effect of molecular size and shape on partitioning are not yet available.

In this paper, we develop a statistical mechanical theory for molecular distributions in interphases that has the aforementioned features. First, we formulate the theory in the framework of the mean-field approximation. Next, the lateral pressure distribution in a model lipid bilayer is calculated via molecular dynamics (MD) simulation. Orientational distributions and relative partition coefficients are obtained as a function of lateral pressure and solute size and shape by solving numerically the relevant equations derived herein. Finally, the mean-field lattice theory developed previously (Marqusee and Dill, 1986) is extended to include the effects of solute size and an additional constraint on partitioning into interphases and compared with our present theory.

STATISTICAL MECHANICAL THEORY

Consider an interphase space V that consists of N_c chain molecules. A Cartesian coordinate system (x, y, z) is defined in the interphase with its z-axis normal to the interface as shown in Fig. 1 for a model lipid bilayer obtained in our present MD simulation (*vide supra*). In the formulation of the theory we shall need the generic molecular distribution func-

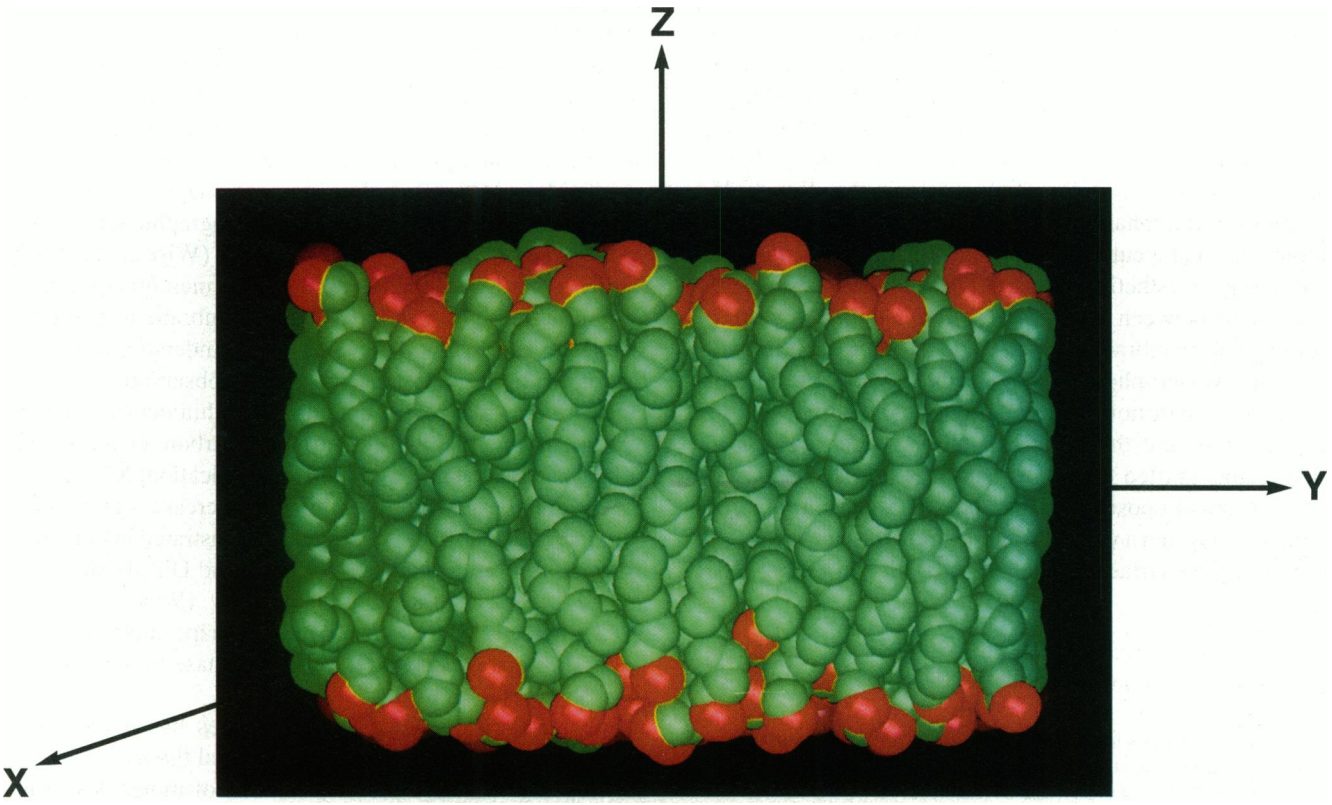

FIGURE 1 Cartesian coordinate system defined in a model lipid bilayer interphase. The bilayer interphase structure with a surface density of 30.5 Å^2/chain was obtained by a MD simulation. It consists of 2 × 100 chain molecules; each chain molecule has 14 methylenes, one methyl, and one head group (red sphere) and is subject to forces restricting bond stretching, bending, and torsional motions.

tion for a solute molecule in the interphase. If there are N_s solute molecules in the interphase, the probability density of finding a solute molecule, say the first solute molecule with a set of coordinates R_1, can be exactly expressed as

$$\rho(R_1) = \frac{\int_V dR_2 \ldots \int dR_{N_s+N_c} e^{-U(R_1,\ldots,R_{N_s+N_c})/k_BT}}{Q(N_s, N_c, V, T)}, \quad (1)$$

where k_B is the Boltzmann constant and T is the absolute temperature. $(R_1, \ldots, R_{N_s})$ and $(R_{N_s+1}, \ldots, R_{N_s+N_c})$ are sets of coordinates for solute and interphase chain molecules, respectively, and R_i itself is a set of coordinates that defines the internal and overall degrees of freedom in molecule i. $Q(N_s, N_c, V, T)$ is the canonical partition function of the overall system. The overall system energy $U(R_1, \ldots, R_{N_s+N_c})$ can be written as

$$U(R_1, \ldots, R_{N_s+N_c}) = U(R_2, \ldots, R_{N_s+N_c}) + U(R_1 | R_2, \ldots, R_{N_s+N_c}) + u_{intl}(\varsigma_1) \quad (2)$$

where $U(R_2, \ldots, R_{N_s+N_c})$ is the overall energy of the subsystem $(2, \ldots, N_s; 1, \ldots, N_c)$, $U(R_1 | R_2, \ldots, R_{N_s+N_c})$ is the interaction energy between solute 1 and all the other molecules in the system and $u_{intl}(\varsigma_1)$ is the internal energy of solute 1, with ς_1 denoting its internal conformation. Furthermore, it is assumed that $U(R_1 | R_2, \ldots, R_{N_s+N_c})$ can be separated into an attractive interaction energy and a repulsive interaction energy

$$U(R_1 | R_2, \ldots, R_{N_s+N_c}) = U_{att}(R_1 | R_2, \ldots, R_{N_s+N_c}) + U_{rep}(R_1 | R_2, \ldots, R_{N_s+N_c}). \quad (3)$$

Before continuing our formulation, two basic assumptions are made: (*a*) The attractive energy $U_{att}(R_1 | R_2, \ldots, R_{N_s+N_c})$ is less sensitive to the coordinates of the surrounding molecules in thermodynamic equilibrium and is thus replaced by an average attractive energy $u_{att}(R_1)$ depending only on the coordinates of molecule 1, and (*b*) the repulsive energy $U_{rep}(R_1 | R_2, \ldots, R_{N_s+N_c})$ is replaced by a hard-core interaction energy, i.e., the overlap of any atom in the subsystem with $V(R_1)$ leads to $U_{rep} = \infty$. Although this assumption is not exact, it is justified by the large slope of the repulsive interaction over a narrow range of interatomic distance. This discontinuous energy acts to constrain the motions of the subsystem $(2, \ldots, N_s; 1, \ldots, N_c)$ within the subspace $V - V(R_1)$, where $V(R_1)$ is the space occupied by molecule 1. Eq. 1 can then be written as

$$\rho(R_1) = \frac{\mathscr{A}}{Q(N_s, N_c, V, T)}. \quad (4)$$

where

$$\mathscr{A} = e^{-[u_{att}(R_1)+u_{intl}(\sigma_1)]/k_BT} \int_{V-V(R_1)} dR_2 \ldots \int_{V-V(R_1)} dR_{N_s+N_c} \cdot e^{-U(R_2,\ldots,R_{N_s+N_c})/k_BT}.$$

The space occupied by molecule 1 depends on the location of its geometrical center (R) and on its configuration (ψ) including internal conformation (ς, which becomes a molecular shape parameter for rigid body solutes) and overall orientation (α, β). For the sake of clarity, the subscript 1 is omitted in the following derivation. Since the interphase is symmetric in the (x, y) domain, any translation of the solute perpendicular to the z-axis does not change the thermodynamic state of the subsystem (N_{s-1}, N_c). Therefore, the probability density, $\rho(R)$, for molecule 1 is a function of its position along the z-axis (Z) and its configuration (ψ), and the multiple integration in Eq. 4 becomes the partition function for the subsystem confined in the space bounded by the walls of the box and the surface of molecule 1, $Q(N_{s-1}, N_c, V - V(Z, \psi), T)$

$$\rho(Z, \psi) = e^{-[u_{att}(Z,\alpha,\beta)+u_{intl}(\varsigma)]/k_BT} \frac{Q(N_s - 1, N_c, V - V(Z, \psi), T)}{Q(N_s, N_c, V, T)}. \quad (5)$$

This thermodynamic state can be reached from a state in which the subsystem (N_{s-1}, N_c) is contained only by the walls of the box at the same temperature by creating reversibly and isothermally an excluded volume $V(Z, \psi)$ in the subsystem. The Helmholtz free energy for the final state is thus a sum of the initial free energy and the reversible work (W) required to create the free volume against a pressure tensor exerted by surrounding molecules

$$-k_BT \ln Q(N_s - 1, N_c, V - V(Z, \psi), T) = -k_BT \ln Q(N_s - 1, N_c, V, T) + W(Z, \psi). \quad (6)$$

From the first and second thermodynamic laws, the reversible work associated with this compression process arises from both entropy and energy contributions, $W = \Delta U - T\Delta S$. For chain molecule interphases, the energy term is associated, in part, with the bending of roughly parallel chain molecules in the neighborhood of molecule 1 in order to avoid passing over the excluded volume (Pace and Datyner, 1979). The entropy term arises from more restricted motions of molecules in the subsystem (N_{s-1}, N_c) as a result of the compression. Because the entropy change associated with translational motions is relatively small (*vide supra*) in comparison with those associated with conformational degrees of freedom, this entropy term is often called the *chain configurational entropy* (Marqusee and Dill, 1986).

To formulate the reversible work W, we refer, in Fig. 2, to a coordinate system defined in the interphase with its origin located at the geometrical center of molecule 1. Consider an infinitesimal surface element within the space $V(Z, \psi)$, $d\mathbf{S}$. Its normal direction is $\mathbf{n}$ (= $\mathbf{r}/r$), where $\mathbf{r}$ is the vector connecting the location of $d\mathbf{S}$ and the origin. The reversible work required to displace this surface element by $d\mathbf{r}$ is $d\mathbf{r} \cdot \mathbf{P} \cdot d\mathbf{S}$, where $\mathbf{P}$ is the pressure tensor

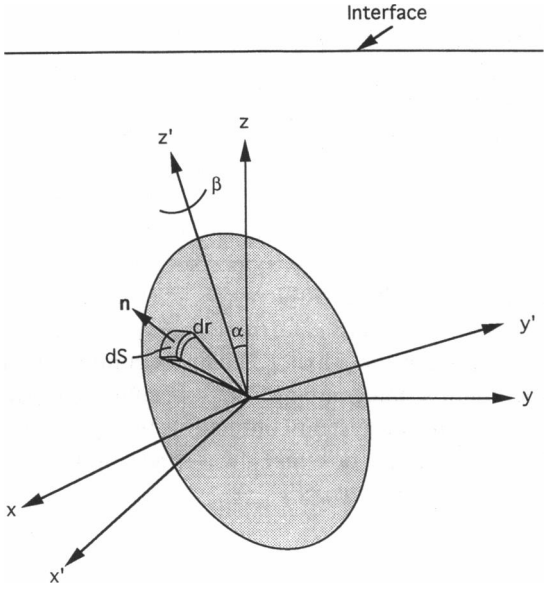

FIGURE 2 Schematic diagram illustrating the rotational transformation of the Cartesian coordinate system defined in the interphase to the Cartesian coordinate system defined in the molecular frame with its z-axis coincident with the molecular long principal axis. The infinitesimal reversible work is to move a surface element $d\mathbf{S}$ over a displacement $d\mathbf{r}$, $\mathbf{n}\cdot\mathbf{P}\cdot\mathbf{n}\, d\mathbf{r}d\mathbf{S}$.

(also called *stress tensor*) (Buff, 1952) exerted by the surrounding interphase molecules. Integrating this work element over the entire volume $V(Z, \psi)$ leads to the total reversible work $W(Z, \psi)$

$$W(Z, \psi) = \int_{V(Z,\psi)} d\mathbf{r}\cdot\mathbf{P}\cdot d\mathbf{S} = \int_{V(Z,\psi)} \mathbf{n}\cdot\mathbf{P}\cdot\mathbf{n}\, dV. \quad (7)$$

In an interphase, the tangential (parallel with the interface) component of the pressure tensor $\mathbf{P}$ may differ from its normal component. Mechanical stability requires that the gradient of this tensor is zero everywhere in the interphase, or

$$\nabla\cdot\mathbf{P} = \mathbf{0} \quad (8)$$

and the symmetry of the interphase requires that the tensor is diagonal with $P_{xx} = P_{yy} = p_\perp$ at any given location. Combining these two conditions, we have

$$\mathbf{P} = \begin{pmatrix} p_\perp & 0 & 0 \\ 0 & p_\perp & 0 \\ 0 & 0 & p_\perp \end{pmatrix}. \quad (9)$$

Since the normal stress component $p_\parallel$ in a planar interphase has the same value irrespective of position and is equal to the pressure of a neighboring bulk phase, it is denoted simply by p.

Substituting Eq. 6 and the following relationship for the chemical potential of solute in the interphase, μ_s,

$$\mu_s = k_BT\left(\frac{\partial \ln Q(N_s, N_c, V, T)}{\partial N_s}\right)_{N_c,V,T} = k_BT \ln [Q(N_s, N_c, V, T)/Q(N_s - 1, N_c, V, T)] \quad (10)$$

into Eq. 5, we have

$$\rho_s(Z, \psi) = e^{-[u_{att}(Z,\alpha,\beta)+u_{intl}(\varsigma)+\mu_s+W(Z,\psi)]/k_BT}. \quad (11)$$

This equation is general in that it applies to the distributions of both solute molecules and molecules composing the interphase. At equilibrium, μ_s is independent of position in the interphase and is equal to the chemical potential of the same species in an adjacent phase, e.g., an aqueous phase,

$$\mu_s = \mu_s(\text{aq}) = \mu^\circ(\text{aq}) + k_BT \ln \rho_s(\text{aq}), \quad (12)$$

where $\mu^\circ(\text{aq})$ and $\rho_s(\text{aq})$ are the standard chemical potential and the probability density of finding the solute species in the aqueous phase, respectively. The standard chemical potential for the solute in the aqueous phase is composed of three components: $\mu^\circ(\text{aq}) = u_{att}(\text{aq}) + u_{intl}(\varsigma) + pV_s$, where $\mu_{cont}(\text{aq})$ is the contact-free interaction energy between the solute molecule and its surrounding solvent molecules, $u_{intl}(\varsigma)$ is the internal energy of the solute, and pV_s is the work required to create a cavity of size equal to the solute volume in the aqueous phase. At an ordinary pressure (p) of 1 bar and temperature of 298 K, the ratio between the work pV_s and the thermal energy k_BT is $2.4 \times 10^{-5}\ V_s$ (Å^3). Thus, one can safely neglect the effect of this work on the solubility of small- and medium-sized solutes in bulk phases.

Substituting Eq. 12 into Eq. 11 and summing the resulting expression over the configurational space of molecule 1, we have the partition coefficient (molar concentration units) of solute between the interphase and a neighboring aqueous phase

$$K_{Z/aq} = \sum_\psi \rho_s(Z, \psi)/\rho_s(\text{aq}) = \sum_\psi e^{-[W(Z,\psi)-pV_s+u_{att}(Z,\alpha,\beta)-\mu_{cont}(\text{aq})]/k_BT}. \quad (13)$$

Many molecular species, notably fluorescent probes, DNAs, and proteins, can be described as rigid bodies that lack internal degrees of freedom. For these solutes, Eq. 13 reduces to

$$K_{Z/aq} = \int_0^\pi \int_0^{2\pi} e^{-[W(Z,\alpha,\beta)-pV_s+u_{att}(Z,\alpha,\beta)-\mu_{cont}(\text{aq})]/k_BT} \sin\alpha\, d\alpha\, d\beta, \quad (14)$$

where the integration is over all orientations of molecule 1 in the interphase. Because of the symmetry of the interphase, the orientation of the solute molecule is uniquely specified by two Euler angles (α, β) involving a rotation in two successive steps as shown in Fig. 2. The first is a rotation of the molecular long axis about the y-axis through an angle α and

the second is a rotation about the new z-axis (molecular long axis) through an angle β.

From Eq. 11, one can obtain the probability density of finding the solute molecule in an orientation state (α, β) as

$$\rho(Z, \alpha, \beta) = \frac{e^{-[W(Z,\alpha,\beta)+u_{att}(Z,\alpha,\beta)]/k_BT}}{\int_0^{\pi}\int_0^{2\pi} e^{-[W(Z,\alpha,\beta)+u_{att}(Z,\alpha,\beta)]/k_BT} \sin\alpha\, d\alpha\, d\beta}. \quad (15)$$

We now consider a general case in which the solute molecule is an ellipsoid characterized by the lengths of the principal axes (a_x, a_y, a_z). The rotation matrix that transforms the coordinate system defined in the interphase frame (x, y, z) (cf. Fig. 2) to the coordinate system defined in the molecular frame, (x', y', z'), is

$$\mathbf{M} = \begin{pmatrix} \cos\alpha\cos\beta & \sin\beta & -\sin\alpha\cos\beta \\ -\cos\alpha\sin\beta & \cos\beta & \sin\alpha\sin\beta \\ \sin\alpha & 0 & \cos\alpha \end{pmatrix}. \quad (16)$$

Since the volume element dV does not vary upon rotational transformation, the reversible work W in Eq. 7 can be written in the molecular frame as

$$W(\alpha, \beta, Z) = \int \mathbf{n}' \cdot \mathbf{MPM}^{-1} \cdot \mathbf{n}'\, dV' = \sum_{u,v=x,y,z} I_{uv}, \quad (17)$$

where

$$I_{uv} = \int_V A_{uv}(\alpha, \beta, p_\perp, p) \frac{u'v'}{x'^2 + y'^2 + z'^2} dx'\, dy'\, dz'. \quad (18)$$

Both I_{uv} and A_{uv} are symmetric with respect to the exchange of u and v, where $u, v = x', y'$, or z'. The parameters A_{uv} are functions of solute orientation (α, β) and the pressure components $p_\perp$ and p in the interphase. Their analytical forms are listed in Table 1. The integration space in the above equation is confined within the surface

$$\frac{x'^2}{a_x^2} + \frac{y'^2}{a_y^2} + \frac{z'^2}{a_z^2} = 1. \quad (19)$$

Transforming the variables (x', y', z') to the new ones $(x'' = x'/a_x, y'' = y'/a_y, z'' = z'/a_z)$ and using a spherical coordinate system for the variables (x'', y'', z''), we have

$$I_{uv} = a_x a_y a_z \cdot \int_0^1 \int_0^{\pi} \int_0^{2\pi} \frac{A_{\mu\nu} a_\mu a_\nu u''v''}{a_x^2 x''^2 + a_y^2 y''^2 + a_z^2 z''^2} \sin\theta''\, d\theta''\, d\phi''\, r''^2\, dr''. \quad (20)$$

Since the lateral pressure $p_\perp$ is a function of depth in the interphase, z, we express z and therefore $p(z)$ in terms of the new coordinate variables (θ'', ϕ'', r'') and the orientational parameters (α, β)

$$z = (-\sin\alpha\cos\beta\sin\theta''\cos\phi'' a_x + \sin\alpha\sin\beta\sin\theta''\sin\phi'' a_y + \cos\alpha\cos\theta'' a_z) r'' + Z \quad (21)$$

where Z denotes the location of the geometrical center of the solute, and substitute it into Eq. 20.

If we assume an effective $p_\perp$ which is constant over the solute dimensions, $p_\perp$ is dependent only on the position Z and the integrand in Eq. 20 is independent of the integration variable r''. Thus, we have

$$I_{uv} = V_s A_{uv} B_{uv} \quad (22)$$

where

$$B_{uv} = \frac{1}{4\pi} \int_0^{\pi} \int_0^{2\pi} \frac{a_u a_v u''v''}{a_x^2 x''^2 + a_y^2 y''^2 + a_z^2 z''^2} \sin\theta''\, d\theta''\, d\phi'' \quad (23)$$

and the solute volume V_s is equal to $\frac{4}{3}\pi a_x a_y a_z$. Substituting Eq. 22 into Eq. 17 yields

$$W(\alpha, \beta, Z, a_x, a_y, a_z) = V_s \sum_{u,v=x,y,z} A_{uv}(\alpha, \beta, Z) \beta_{uv}(a_x/a_y, a_x/a_z). \quad (24)$$

Equation 24, in combination with Eqs. 14 and 15, gives the analytical forms for the dependence of molecular distribution in an interphase on various solute dimension and orientation parameters.

For a spherical solute, Eq. 24 reduces to

$$W(Z) = \tfrac{1}{3}(p + 2p_\perp(Z))V_s \quad (25)$$

which, upon substitution into Eq. 14, gives

$$K_{Z/aq} = e^{-[(2/3)(p_\perp(Z) - p)V_s + u_{att}(Z) - u_{cont}(aq)]/k_BT}. \quad (26)$$

This result shows that the bulk solvent/interphase partition coefficient is an exponential function of solute volume. Since, as to be shown below, the effect of molecular shape on partitioning into an interphase is relatively weak, Eq. 26 provides a simple and reasonably accurate expression for the effect of solute size on partitioning even though the solute may be elongated.

For a solute molecule with arbitrary shape and flexibility such as a chain molecule at a given conformation, an exact

TABLE 1 Analytical forms for all the components of the orientation parameters A_{uv}^*

$A_{xx} = p_\perp - \sin^2\alpha\cos^2\beta(p_\perp - p)$
$A_{yy} = p_\perp - \sin^2\alpha\sin^2\beta(p_\perp - p)$
$A_{zz} = p_\perp - \cos^2\alpha(p_\perp - p)$
$A_{xy} = \sin^2\alpha\sin\beta\cos\beta(p_\perp - p)$
$A_{xz} = \sin\alpha\cos\alpha\cos\beta(p_\perp - p)$
$A_{yz} = -\sin\alpha\cos\alpha\sin\beta(p_\perp - p)$

* $A_{uv} = A_{vu}$.

evaluation of the reversible work in Eq. 7 can be undertaken by the following numerical procedure. First, a rectangular cell having the minimum area necessary to envelope the solute molecule is created by sorting atom by atom the locations of atoms that have the largest absolute displacements from the geometrical center of the solute molecule in the x, y, or z direction. Once the box is set up, a sufficiently large number of random number arrays $\{x_i, y_i, z_i, i = 1, 2, \ldots, N\}$ are generated to uniformly select locations in the box. If a location is occupied by an atom in the molecule, the unit vector (**n**) that joins this position and the geometrical center of the molecule are determined and used to calculate the quantity $\mathbf{n} \cdot \mathbf{P} \cdot \mathbf{n}$. The reversible W then becomes

$$W = \frac{V_0}{N} \sum n_i \cdot P_t \cdot n_t \tag{27}$$

where V_0 is the volume of the cell enclosing the solute molecule.

Regardless of the complexity of the solute molecule, the only physical parameter required for a quantitative prediction of solute distribution in an interphase is the lateral pressure profile in the interphase. This quantity can be obtained through the following two approaches: (*a*) a full-scale MD simulation of the interphase or (*b*) a self-consistent statistical mechanical calculation in which various molecular conformations for flexible chain molecules or overall orientations for rigid-body molecules are sampled by a Monte Carlo method as lateral pressure is varied. Overall or local segmental order parameters calculated using the equations derived above are then compared with deuterium magnetic resonance, anisotropic fluorescence, and other experimental measurements to determine the lateral pressure yielding the experimental order parameters (Mulders et al., 1986; Seelig and Seelig, 1974). The first approach is used in the following section to estimate the lateral pressure profile in a model lipid bilayer.

Lateral pressure as a function of depth in a model lipid bilayer—MD simulation

If the nonbond intermolecular interaction is pairwise, the lateral pressure distribution in a planar interphase can be calculated from a formula derived by Kirkwood and Buff (1949) and Harasima (1958),

$$p_\perp(z) = \frac{1}{4V(z)} \left\langle \sum_{i \subset (z-\delta z/2,\, z+\delta z/2)} \sum_{j\, i} \frac{du}{dr_{ij}} \frac{x_{ij}^2 + y_{ij}^2}{r_{ij}} \right\rangle - \frac{k_B T N(z)}{V(z)}, \tag{28}$$

where $N(z)$ and $V(z)$ ($= A\delta z$, A is the total area of the interphase in the plane parallel with the interface and δz is the increment along the z-axis) are the number of molecules and volume increment at position z in the interphase, respectively. The angled brackets stand for an ensemble average, which will be replaced by an average over time taking the advantage of the ergodicity of a thermodynamic system. In Eq. 28 use has been made of the relation that the lateral pressure $p_\perp$ is the negative of the tangential component of the pressure tensor, $-p_T$, as defined in the literature (Rowlinson and Widom, 1982).

The lateral pressure profile in a model lipid bilayer is calculated using the above equation and a given microstructure (a set of Cartesian coordinates for all the chain segments) of the bilayer, which was obtained from MD simulation. A detailed description of the simulation procedure has been published elsewhere (Xiang, 1993). In brief, a large bilayer assembly with 2×100 lipid molecules was simulated, in which the bilayer was confined in a unit box with periodic boundary conditions in the x–y domain. Each chain molecule had 14 methylene, one methyl, and one head group. All groups were treated as single spheres and were subject to the forces restricting bond stretching, bending, and torsional motions (Xiang et al., 1991). The Rychaert-Bellemans potential (Rychaert and Bellemans, 1975) was used for torsional motions of the C-C-C-C linkages (ϕ). The Lennard-Jones (12–6) potential was employed for intermolecular interactions and for interactions between segments separated by more than three bonds in the same molecule. The surface density (30.5 Å^2/chain molecule) was chosen such that the segmental order parameters calculated were in close agreement with experimental values for dipalmitoyl phosphatidylcholine bilayers at 323 K (Seelig and Seelig, 1974). The head group, the same size as a carboxylate group, was anchored to a mobile plane by a harmonic force. This simplification substantially reduced the CPU time expended on head groups and the neighboring water phase. The force constant for the anchoring of the head groups was 4.5 kJ/mol Å^2. A pressure of 1 bar was exerted on the head groups normal to the bilayer interface. The equations of motion were integrated by using the Verlet algorithm and a time step of 2 fs. A snapshot of the bilayer structure is shown in Fig. 1.

Since the attractive and repulsive components of the L–J (12–6) force are additive, we can explore their relative contributions to the overall lateral pressure. Fig. 3 shows the three components (pressure due to kinetic motion, intermolecular attractive force, and intermolecular repulsive force) of the lateral pressure distribution in the model lipid bilayer versus the distance from the center of the bilayer ($Z = 0$). The overall lateral pressure in the bilayer is plotted in Fig. 4. Because of the large statistical fluctuations in lateral pressure obtained from a single microstructure, the reported lateral pressure is an average over 200 microstructures separated from one another by 0.2 ps. Several important results are noted. First, the repulsive and attractive contributions to the lateral pressure are both very large and roughly equal in magnitude but opposite in direction. The slight dominance of attractive over repulsive forces is responsible for the cohesion and stability of the lipid bilayer. Second, the lateral pressure has a plateau value of 309 ± 48 bar in the highly ordered region and decreases abruptly near the center of the bilayer. The drastic difference between the lateral pressure in the highly ordered region and the pressure of 1 bar normal to the bilayer interface is in accordance with the

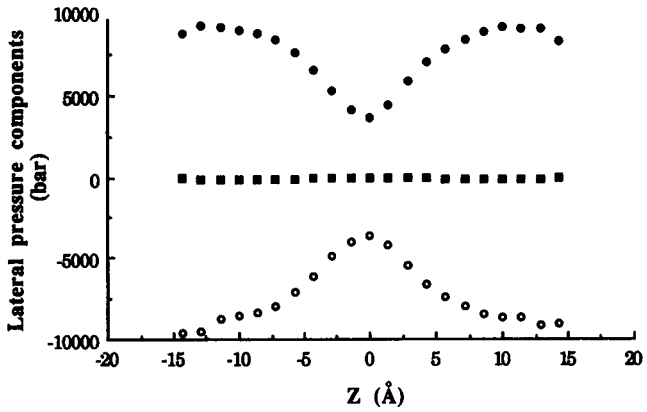

FIGURE 3 The three components, molecular kinetic motion (■), intermolecular attractive force (●), and intermolecular repulsive force (○), of the lateral pressure distribution in the model lipid bilayer versus the distance from the center of the bilayer. The microstructures (Cartesian coordinates of the chain segments in the bilayer) of the bilayer assembly were obtained from the present MD simulation.

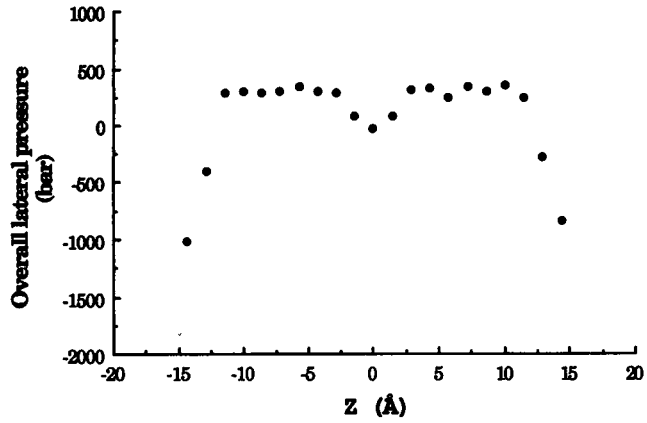

FIGURE 4 The overall lateral pressure in the model lipid bilayer versus the distance from the center of the bilayer.

physical intuition that there is a much higher probability for a chain segment to be located adjacent to a neighboring chain segment belonging to a different chain molecule in the (x, y) domain than along the z direction in the highly ordered chain region. In the regions very close to the interfaces, the lateral pressure declines sharply, becoming negative. While it is likely that the head groups do exert a considerable negative lateral pressure (Gruen, 1980), taking into account interactions between head groups and head group–water interactions is extremely difficult. A full account should include interactions between head groups (e.g., electrostatic and hydrogen bonding), increased packing density, increased ordering of water molecules in the interface due to interactions with head groups, and repulsive interactions among molecules in the interface. The present model did not take these factors into account, and therefore the negative lateral pressures obtained are purely boundary artifacts.

Since the lateral pressure near the interface is ill determined, and the distribution is symmetric with respect to the midplane of the bilayer ($Z = 0$), we discarded the two data points near the interface, averaged the data points at the symmetric positions in each monolayer, and fit the resulting data points to several model equations using the method of least squares. The best model, as described by Eq. 29,

$$p_\perp(Z) = a_1(1 - e^{-a_2 Z^2}) + a_3 \tag{29}$$

was chosen based on a modified Akaike Information Criterion, which places a burden on the model with more parameters. The results for the three adjustable parameters, a_1, a_2, and a_3, were $a_1 = 347 \pm 25$ bar, $a_2 = 0.26 \pm 0.06$ Å^{-2}, and $a_3 = -38 \pm 23$ bar with a correlation coefficient of 0.99. In Eq. 29, a_3 is the lateral pressure in the center of the bilayer, and $a_1 + a_3$ is the lateral pressure in the highly ordered plateau region. a_2 measures the steepness of the change in lateral pressure from the midplane toward the interface region in the bilayer.

The lateral pressure is related to the surface tension, γ, in the bilayer by the following expression (Rowlinson and Widom, 1982),

$$\gamma = \int_0^{z_i} [p_\perp(Z) - p]\, dZ \tag{30}$$

where z_i is the location of the monolayer interface. From the lateral pressure profile calculated above we obtain $\gamma_{hc} = 27.6$ dyn/cm, a value that is very close to the surface tension of 27.3 dyn/cm in the hydrocarbon chain region in a dipalmitoyl phosphatidylcholine lipid bilayer used by Gruen (1980) in a statistical mechanical calculation to fit experimental order parameters (Seelig and Seelig, 1974).

In the following two sections, the effects of excluded volume interactions, as expressed by the reversible work, on the orientational distribution and relative partition coefficient of solute in an interphase are examined as the anisotropy of the mean attractive interaction energy plays a somewhat secondary role (Meraldi and Schlitter, 1981; Warner, 1980).

Outcomes of statistical mechanical theory

Orientational distribution

We now consider the effect of excluded volume interactions on the orientational distribution of rodlike molecules (e.g., chain molecules having close to an all-*trans* conformation) in an interphase. These molecules can be modeled as ellipsoids with $a_x = a_y$. Thus, only one Euler angle, α, the angle between the z-axis in the interphase coordinate system and the principal axis, a_z, defined in the solute molecule, uniquely defines its orientation in the interphase (cf. Fig. 2). Fig. 5 shows the probability density for the orientation angle α versus the second Legendre polynomial, $(3\cos^2\alpha - 1)/2$, at several values of lateral pressure. The solute molecule has a volume of 100 Å^3 in Fig. 5 *a* and 300 Å^3 in Fig. 5 *b*. The axial ratio a_z/a_x for the solute is fixed at 3.0 in both figures. As noted, in all the situations the most favorable orientation is at $\alpha = 0°$, i.e., when the molecular long axis aligns normal to the interface. The log probability density increases linearly

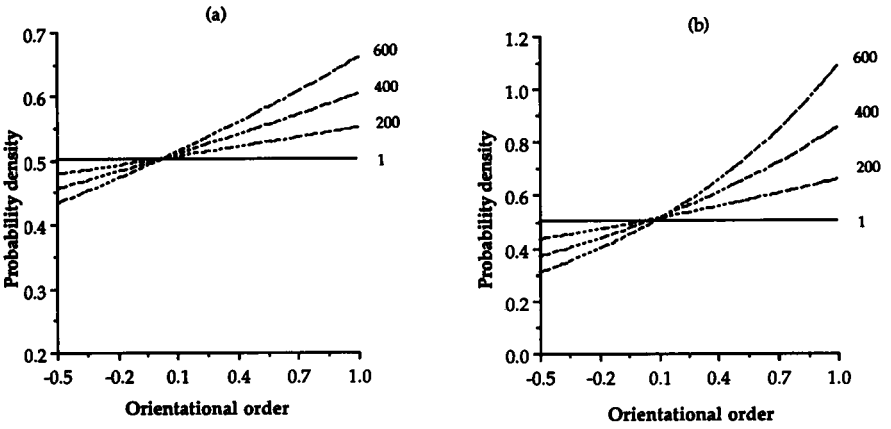

FIGURE 5 The probability density for the orientation angle α between the molecular long axis and the normal to the interface versus the orientational order, $(3\cos^2\alpha - 1)/2$, at several values of the lateral pressure (shown in the figures in a unit of bar). The solute molecule has a volume of 100 Å^3 in (a) and 300 Å^3 in (b). The axial ratio a_z/a_x for the solute is fixed at 3.0 in both figures.

with the orientational order with a slope proportional to two-thirds of the lateral pressure $p_\perp$. The selected values of the lateral pressure are realistic as shown in our MD simulation (cf. Fig. 4) along with the fact that the surface tension varies substantially with surface density (White and King, 1985). At a lateral pressure of 1 bar, which corresponds to an isotropic bulk phase, the probability density becomes independent of molecular orientation.

The average molecular orientation in an interphase can be characterized by the order parameter S_α

$$S_\alpha = \frac{1}{2}(3\langle\cos^2\alpha\rangle - 1) = \frac{1}{2}\left(3\int \cos^2\alpha P(\alpha)\sin\alpha\, d\alpha - 1\right) \quad (31)$$

The effect of molecular shape on solute orientation in an interphase is illustrated in Fig. 6, where the order parameters for solutes with a fixed volume of V_s = 100 or 300 Å^3 are plotted as a function of axial ratio, a_z/a_x, at several lateral pressures. Order parameters increase with both the axial ratio and the lateral pressure in the interphase. The trends shown in Fig. 6 are more pronounced for larger solute molecules, consistent with the experimental findings that the larger fluorescent probe, 1-[4-(trimethylammonium)phenyl]-6-phenyl-1,2,5-hexatriene, has a greater orientational order than the smaller molecule, 1,6-diphenyl-1,3,5-hexatriene, in phospholipid bilayers above their phase transitions (Mulders et al., 1986). Deuterium nuclear magnetic resonance measurements (Pope et al., 1984) have also shown that chain molecules (n-alkanes and n-alkanols) dissolved in phospholipid bilayers have order parameters corresponding to their favorable alignment along the normal to the interface, with the order parameter for n-dodecane (0.14) being greater than those for n-octane (0.11) and n-hexane (0.09), both having smaller volumes and axial ratios than n-dodecane.

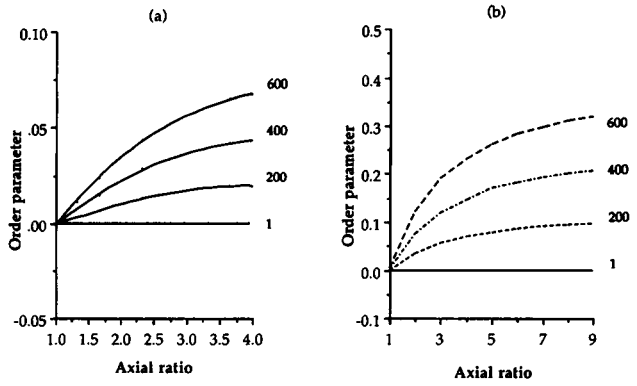

FIGURE 6 The order parameter for solute with a fixed volume of V_s = 100 Å^3(a) and 300 Å^3 (b), respectively, versus its axial ratio, a_z/a_x, at several values of the lateral pressure (shown in the figures in the unit of bar).

Partition coefficients

An expression similar to Eq. 14 can be derived for the partition coefficient of solute between an organic solvent and an aqueous solution, which, upon substitution into Eq. 16, gives

$$K_{Z/aq} = \zeta K_{org/aq} \quad (32)$$

where

$$\zeta = e^{-[\mu_{att}(Z)-\mu_{cont}(org)]/k_BT} \times \int_0^{\pi}\int_0^{2\pi} e^{-[W(Z,\alpha,\beta)-pV_s]/k_BT}\sin\alpha\, d\alpha\, d\beta \quad (33)$$

In Eq. 33, μ_{cont}(org), the contact energy for the solute in the organic solvent, is independent of solute orientation due to the isotropic nature of the bulk organic phase. $\mu_{att}(Z) - \mu_{cont}$(org) accounts for the difference of chemical microenvironment between the interphase at Z and the bulk organic solvent. If the organic solvent chosen closely mimics the microenvironment of the interphase, Eqs. 32–33 predict that the interphase/water partition coefficients for a series of solutes having similar molecular dimensions would correlate approximately linearly with their organic solvent/water partition coefficients. This idea has been utilized in experiments to explore the polarity of the transport barrier domain in lipid bilayers (Xiang and Anderson, submitted for publication;

Xiang et al., 1992). However, even when the interphase is composed of hydrocarbon chains and a hydrocarbon solvent is used as a reference organic phase, $\mu_{cont}(Z)$ may differ from $\mu_{cont}(org)$ in two respects. First, MD simulations of a model lipid bilayer (Xiang, 1993) have shown that local segmental density varies with depth in the bilayer. Since the *vdW* dispersion energy depends on average molecular separation d ($\propto 1/d^5$) (Salem, 1962), $u_{att}(Z)$ may also change with distance from the interface. Secondly, $u_{att}(Z)$ is likely to be altered by the significant dipole potential that exists across the hydrophobic interior of bilayers due to the partial charge distribution in the polar regions (Flewelling and Hubbell, 1986; Zheng and Vanderkooi, 1992).

The steric partitioning behavior of solutes in interphases is investigated in Figs. 7 and 8. Fig. 7 shows that the partition coefficients of spherical solutes decrease exponentially with solute volume. The slope of the log partition coefficient versus molecular volume plot is proportional to two-thirds of the lateral pressure, in contrast to the direct proportionality previously suggested (Carignano and Szleifer, 1993). The decrease in partition coefficient with increasing lateral pressure is in accordance with the observation that increasing surface density leads to expulsion of solute from lipid bilayers (DeYoung and Dill, 1988, 1990).

Fig. 8 shows the relative partition coefficient versus the solute axial ratio at several lateral pressures, for a solute having a fixed volume of 300 Å^3. The relative partition coefficient increases with the axial ratio at a constant volume, indicating that the interphase exhibits an extra discrimination against branched solutes over straight-chain homologues having the same chemical nature. This is consistent with experimental observations for the partitioning of branched versus straight-chain alkanols in lecithin bilayers (Diamond and Katz, 1974). It should be noted, however, that compared with the effect of solute volume on partitioning into the interphase, molecular shape effects play a minor role. This can be rationalized by the fact that even though the energetics of the system and the configurational entropy of the surrounding molecules favor the orientation of a solute with its long

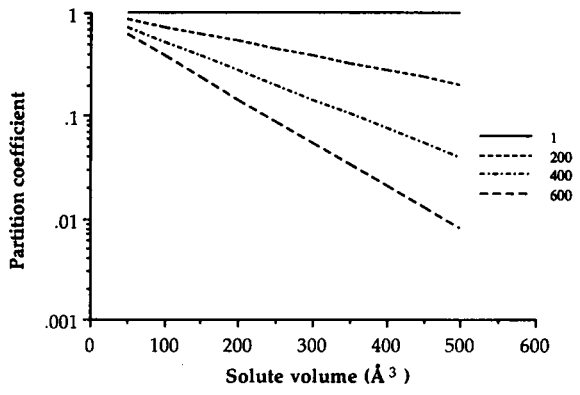

FIGURE 7 The relative steric partition coefficient for spherical solute into an interphase versus its molecular volume at several values of the lateral pressure (shown in the figure in the unit of bar).

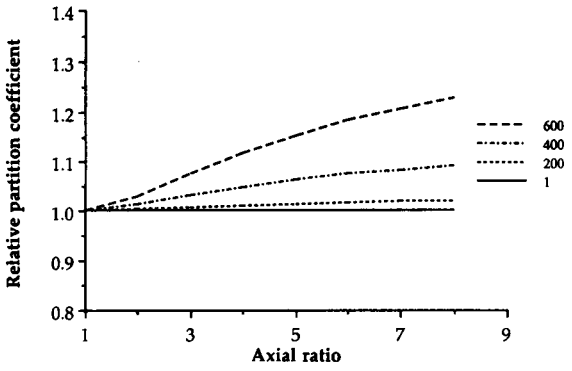

FIGURE 8 The relative partition coefficient versus the axial ratio of the solute at several values of the lateral pressure (shown in the figure in the unit of bar), given that the solute has a fixed volume of 300 Å^3.

axis aligned normal to the surface, as shown in Figs. 5 and 6, it is unfavorable in terms of orientational entropy of the solute molecule itself because the orientational space approaches zero when the solute aligns normal to the interface.

We have recently explored experimentally the physicochemical nature of transport barriers and the relationship between permeability and solute size in egg PC bilayer membranes (Xiang et al., 1992; Xiang and Anderson, submitted for publication). It has been found that the highly ordered hydrocarbon chain region is the rate-limiting domain resembling the microenvironment of 1,9-decadiene bulk solvent, and the permeability coefficients, being proportional to the product of the diffusion coefficients in and the partition coefficients into the barrier domain in the bilayer, can be modeled by an equation that combines an empirical relationship for size selectivity of diffusion, $1/V^n$, and Eq. 28 for size selectivity of partitioning. The lateral pressure of 300 ± 100 bar was obtained from the data analysis (Xiang and Anderson, submitted for publication), which is in close agreement with the lateral pressure in the highly ordered region in our model lipid bilayer, 309 ± 48 bar. The egg lecithin bilayer has an average chain length of 17.8 carbons and the same surface density as the simulated bilayer (Fettiplace et al., 1971).

Using the lateral pressure profile obtained in the present MD simulation, we calculated relative partition coefficients for *n*-hexane in the hydrocarbon chain region of our model bilayer as a function of distance from the center of the bilayer. The results are shown in Fig. 9. Since, as shown in Fig. 8, the membrane partition coefficient is only weakly dependent on solute shape, *n*-hexane was modeled as an ellipsoid with a volume of 113 Å^3 and an axial ratio of 2.5 (approximating an all-*trans* conformation). The volume was estimated by the atomic increment method (Edward, 1970), and the axial ratio was estimated with the aid of a molecular graphics program (InsightII 2.2.2; Biosym Technologies, San Diego, CA). The results in Fig. 9 correctly predict that hexane is more concentrated in the center of the bilayer, as small-angle neutron scattering experiments by White et al. (1981) have confirmed.

Comparison with lattice theory

Equation 26 for partitioning of globular molecules into interphases is formally analogous to the expression developed by Marqusee and Dill (1986) in the framework of a mean-field lattice theory

$$K_{i/aq} = e^{-\lambda_i - [\mu_{att}(i) - \mu_{cont}(aq)]/k_BT} \tag{34}$$

where λ_i ($i = 1, 2, \ldots, L$) is a Lagrange multiplier at layer i. In their analysis, the solute was assumed to have the same size as a lattice site. The Lagrange multiplier λ_i was related to the lateral pressure at layer i by $\lambda_i = p_\perp V_c/k_BT$ (Carignano and Szleifer, 1993), where V_c is the volume of a lattice site. The fundamental difference between our present formulation in the limit of spherical solutes and Eq. 34 is the presence of a factor of ⅔ in Eq. 26. The physical implication of this factor is that the lateral pressure is defined and thereby acts only on a two-dimensional space. Since the lateral pressure is usually much greater than the normal pressure component (e.g., 1 bar), Eq. 34 would overestimate substantially the effect of interphase chain packing on solute distributions in interphases. The discrepancy may arise from the fact that in the derivation of Eq. 34, only space-filling constraints in the (x, y) domain have been considered.

We now extend Dill's lattice model to account for the effects of solute size on solute partitioning into an interphase. The planar interphase consists of N_c hydrocarbon chain molecules and is modeled as a cubic lattice divided into L layers parallel with the interface. Each chain is composed of n lattice segments occupying contiguous sites on the lattice. The linear dimension of each lattice site is equal to 3.6 methylene groups, which corresponds to the width of the chain and a volume of $V_c = 97.3$ Å^3 for each lattice site. The first segment of a chain molecule is anchored at the first layer. The chemical potential for a solute in the interphase at layer i, $\mu_s(i)$, can be written as

$$\mu_s(i) = \mu^0(i) + \mu_c(i) + k_BT \ln \rho_s(i) \tag{35}$$

where $\mu^0(i)$ includes the mean interaction energy between the solute at layer i and its surroundings and ρ_i is the molar concentration of the solute in layer i. The third term arises from the entropy of mixing and is derived in the framework of the Flory-Huggins (FH) theory (Flory, 1942; Huggins, 1942). For mixtures of global molecules with chain molecules, the FH theory is appropriate (Flory, 1970; Rowlinson, 1970). The second term is an extra entropy due to the perturbation of chain conformations in the interphase in the presence of solute. The conformational entropy S_c associated with this effect can be expressed as

$$S_c = -k_BN_c \sum_{\mathbf{l}} P(\mathbf{l}) \ln\left[\frac{P(\mathbf{l})}{g(\mathbf{l})}\right] \tag{36}$$

where $\mathbf{l} = (l_1, l_2, \ldots, l_n)$ is a sequence of layers in which the chain segments $\{k = 1, 2, \ldots, n\}$ occur. $P(\mathbf{l})$ is the probability for the conformation $\mathbf{l}$ and $g(\mathbf{l})$ is the degeneracy of the conformation $\mathbf{l}$. The chain molecules are assumed to fill

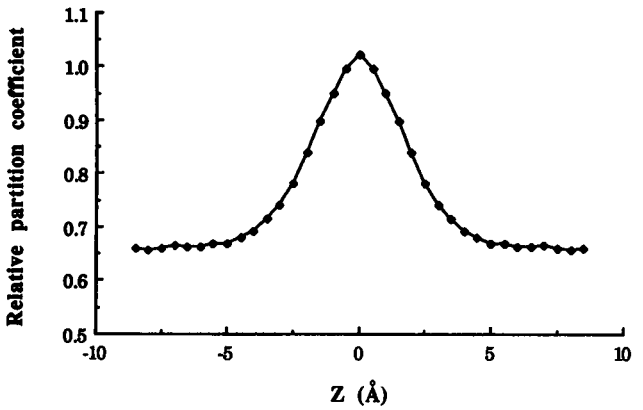

FIGURE 9 The relative partition coefficient distribution for n-hexane in a model lipid bilayer. The bilayer microstructure was obtained by means of MD simulation. The partition coefficient in the center of the bilayer is assumed to be 1.

all the space of the interphase, and thus $P(\mathbf{l})$ must meet the packing constraints

$$\frac{N_o}{N_c} = \sum_l n_i(l)P(l) \tag{37}$$

where $i = 1, 2, \ldots, L$, and the following two conservation conditions

$$\sum_i^L \sum_l n_i(l)P(l) = \frac{LN_o}{N_c} = n \tag{38}$$

$$\sum_l P(l) = 1 \tag{39}$$

where N_o is the number of sites in each layer and $n_i(\mathbf{l})$ is the number of segments in the layer i when the chain has the conformation $\mathbf{l}$. Eq. 38 is not redundant because it constrains the total number of layers L in each monolayer in the bilayer.

Maximizing the conformational entropy S_c in Eq. 36 subject to the above constraints and assuming that there are $n_s(i)$ solutes in layer i, which occupy approximately $V_sn_s(i)/V_c$ lattice sites in layer i, we have (Marqusee and Dill, 1986)

$$\frac{N_o - V_sn_s(i)/V_c}{N_c} = -\frac{\partial \ln Q}{\partial \lambda_i} \tag{40}$$

and

$$\sum_i^L \frac{N_o - V_sn_s(i)/V_c}{N_c} = -\frac{\partial \ln Q}{\partial \kappa_i} \tag{41}$$

where

$$Q = \sum_l g(l) \prod_i^L e^{-n_i(\lambda_i + \kappa)} \tag{42}$$

and λ_i and κ are the Lagrange multipliers. Since λ_i and κ are conjugate variables of N_o and L, from dimensional analysis, λ_i is proportional to the lateral pressure whereas κ is proportional to the normal pressure in the interphase. Moreover,

because of the mechanical stability of the interphase, κ is independent of location in the interphase. Eq. 36 can then be written as

$$\frac{S_c}{k_B} = N_c \ln Q - \sum_{i=1}^{L} \left(N_o - \frac{V_s n_s(i)}{V_c} \right) (\lambda_i + \kappa). \quad (43)$$

The contribution of the configurational entropy (S_c) to the chemical potential of solute in the interphase can be written as

$$\mu_c(i) = -T \left(\frac{\partial S_c}{\partial n_s(i)} \right)_{T,N_c,N_o,n_s(j\,i)} \quad (44)$$

which, combining with Eqs. 40–43, yields (Marqusee and Dill, 1986)

$$\mu_c(i) = -(\lambda_i + \kappa) V_s / V_c. \quad (45)$$

Following the same procedure from Eq. 11 to Eq. 13, we can express the partition coefficient between the aqueous phase and layer i in the interphase as

$$K_{Z/aq} = e^{-[\lambda_i' V_s / V_c + (\mu_{att}(i) - \mu_{conf}(aq))/k_B T]} \quad (46)$$

where $\lambda_i' = \lambda_i + \kappa$. λ_i' is identical to the λ_i values previously evaluated (Marqusee and Dill, 1986) provided that the total number of layers in a monolayer is chosen to satisfy the constraint Eq. 38. It is noted, however, that most of the λ_i values listed in Table I in Marqusee and Dill (1986) are determined under conditions that do not satisfy Eq. 38. We calculate λ_i versus i at several surface densities and find that their values vary significantly with the total number of layers in the monolayer L and thereby with whether or not the constraint Eq. 38 is imposed on the calculation. When the total number of layers is greater than what is required to fill all the lattice sites, larger values of λ_i (lateral pressures) are obtained.

It is important to be aware of the assumptions made in the above analysis, which may limit the degree to which lattice theory can be applied to problems involving real interphases. First, the lattice site length is equal to 3.6 methylene segments in a chain molecule, and thus the chain conformations are restricted to those that fully occupy contiguous lattice sites. Only bond angles of 0, $\pi/2$, and π with respect to the interphase normal are allowed. Second, the density throughout the interphase is assumed to be a constant. This condition is necessary to establish the space-filling constraints (i.e., Eqs. 37 and 38) on the basis of which various interphase properties can be calculated. In this approximation, the total volume for each layer is determined solely by the geometrical factor of the interphase. However, this approximation is valid only for interphases with very high surface density (Murat and Grest, 1989). For lipid bilayers at lower surface densities of biological relevance, our recent studies have revealed that the segmental density (or free volume fraction) varies roughly parabolically with distance from the surface (Xiang, 1993). Similar results have been obtained in grafted polymer systems (Murat and Grest, 1989), and a variable-density lattice theory for polymer melt/solid interfaces has recently been developed (Theodorou, 1989). Third, the binding energy associated with each chain conformation is either discarded or incorporated into the model in a phenomenological manner. Moreover, the identification of 3.6 chain segments as a lattice cell unit causes difficulty in relating binding energy to experimental quantities. Finally, the first segment of each chain molecule in the lattice is anchored to the surface. In real bilayer interphases, the position of the first segment may fluctuate perpendicularly to the bilayer surface with a width on the order of 4 Å (Wiener and White, 1992). Artificially high apparent chain ordering may result from neglecting interfacial fluctuations (unpublished result).

CONCLUSIONS

A statistical mechanical theory has been proposed that relates explicitly various distribution properties of solute within an interphase (including the interphase molecule itself) to molecular structure of solute as characterized by size, shape, orientation and other internal degrees of freedom and to the interphase structure as characterized by its lateral pressure as a function of depth. Once a solute or interphase molecule is chosen, lateral pressure as obtained from MD simulations and the solute-solvent interaction constants (e.g., the Flory (1953) interaction parameter) are the few parameters required to calculate various distributions in the interphase. The driving forces for solute distribution in an interphase include the interaction energy between the solute and its surrounding molecules, and the reversible work required to create a cavity of size equal to the solute volume, which includes the configurational entropy and the binding energy of the surrounding interphase molecules. The reversible work for cavity formation is governed by the lateral pressure in an interphase, which may be substantially higher than that in bulk phases. Compared with the mean-field lattice theory, our present theory has several major advantages. First, the theory is general and applicable to real physical systems. Second, not only size but shape effects on solute partitioning, orientation, and other physical properties as a function of depth into an interphase can be explored.

This work was supported in part by the Faculty Research Grant (to Dr. T-X. Xiang) from the University of Utah and a research grant (to Dr. B. D. Anderson) from Glaxo, Inc.

REFERENCES

Ben-Shaul, A., I. Szleifer, and W. M. Gelbart. 1984. Statistical thermodynamics of amphiphile chains in micelles. *Proc. Natl. Acad. Sci. USA.* 81:4601–4605.

Buff, F. P. 1952. Some considerations of surface tension. *Z. Elektrochem.* 56:311–313.

Carignano, M. A., and I. Szleifer. 1993. Statistical thermodynamic theory of grafted polymeric layers. *J. Chem. Phys.* 98:5006–5018.

Davis, S. S., T. Higuchi, and J. H. Rytting. 1974. Determination of thermodynamics of functional groups in solutions of drug molecules. *In* Advances in Pharmaceutical Sciences. H. S. Bean, A. H. Beckett, and J. E. Carless, editors. Academic Press, London. 73–261.

DeYoung, L. R., and K. A. Dill. 1988. Solute partitioning into lipid bilayer membranes. *Biochemistry.* 27:5281–5289.

DeYoung, L. R., and K. A. Dill. 1990. Partitioning of nonpolar solutes into bilayers and amorphous *n*-alkanes. *J. Phys. Chem.* 94:801–809.

Diamond, J. M., and Y. Katz. 1974. Interpretation of nonelectrolyte partition coefficients between dimyristoyl lecithin and water. *J. Membr. Biol.* 17: 121–154.

Dill, K. A. 1987. The mechanism of solute retention in reversed phase liquid chromatography. *J. Phys. Chem.* 91:1980–1988.

Dill, K. A., and P. J. Flory. 1980. Interphases of chain molecules: monolayers and lipid bilayer membranes. *Proc. Natl. Acad. Sci. USA.* 77: 3115–3119.

Dill, K. A., and P. J. Flory. 1981. Molecular organization in micelles and vesicles. *Proc. Natl. Acad. Sci. USA.* 78:676–680.

Dill, K. A., J. Naghizadeh, and J. A. Marqusee. 1988. Chain molecules at high densities at interfaces. *Annu. Rev. Phys. Chem.* 39:425–461.

Edward, J. T. 1970. Molecular volumes and the Stokes-Einstein Equation. *J. Chem. Educ.* 47:261–270.

Fettiplace, R., D. M. Andrews, and D. A. Haydon. 1971. The thickness, composition and structure of some lipid bilayer natural membranes. *J. Membr. Biol.* 5:277–296.

Flewelling, R. F., and W. L. Hubbell. 1986. The membrane dipole potential in a total membrane potential model. *Biophys. J.* 49:541–552.

Flory, P. J. 1942. Thermodynamics of high polymer solutions. *J. Chem. Phys.* 10:51–61.

Flory, P. J. 1953. Principles of Polymer Chemistry. Cornell University Press, New York.

Flory, P. J. 1970. Thermodynamics of polymer solutions. *Faraday Discuss. Chem. Soc.* 49:7–29.

Giddings, J. C., E. Kucera, C. P. Russell, and M. N. Myers. 1968. Statistical theory for equilibrium distribution of rigid molecules in inert porous networks. Exlusion chromatography. *J. Phys. Chem.* 72: 4397–4408.

Gruen, D. W. R. 1980. A statistical mechanical model of the lipid bilayer above its phase transition. *Biochim. Biophys. Acta.* 595:161–183.

Harasima, A. 1958. Molecular theory of surface tension. *Adv. Chem. Phys.* 1:203–237.

Hermann, R. B. 1972. Theory of hydrophobic bonding. II. the correlation of hydrocarbon solubility in water with solvent cavity surface area. *J. Phys. Chem.* 76:2754–2759.

Huggins, M. L. 1942. Thermodynamic properties of solutions of long-chain compounds. *Ann. N.Y. Acad. Sci.* 43:1–32.

Kirkwood, J. G., and F. P. Buff. 1949. The statistical mechanical theory of surface tension. *J. Chem. Phys.* 17:338–343.

Lieb, W. R., and W. D. Stein. 1986. Simple diffusion across the membrane bilayer. *In* Transport and Diffusion across Cell Membranes. W. D. Stein, editor. Academic Press, Inc., Orlando, FL. 69–112.

Marqusee, J. A., and K. A. Dill. 1986. Solute partitioning into chain molecule interphases: monolayers, bilayer membranes, and micelles. *J. Chem. Phys.* 85:434–444.

Meraldi, J-P., and J. Schlitter. 1981. A statistical mechanical treatment of fatty acyl chain order in phospholipid bilayers and correlation with exerimental data. A. Theory. *Biochim. Biophys. Acta.* 645: 183–192.

Mulders, F., H. van Langen, G. van Ginkel, and Y. K. Levine. 1986. The static and dynamic behaviour of fluorescent probe molecules in lipid bilayers. *Biochim. Biophys. Acta.* 859:209–218.

Murat, M., and G. S. Grest. 1989. Interaction between grafted polymeric brushes: a molecular-dynamics study. *Phys. Rev. Lett.* 63:1074–1077.

Naghizadeh, J., and K. A. Dill. 1991. Statistical mechanics of chain molecules at interfaces. *Macromolecules.* 24:1768–1778.

Ogston, A. G. 1958. The spaces in a uniform random suspension of fibers. *Trans. Faraday Soc.* 54:1754–1757.

Pace, R. J., and A. Datyner. 1979. Statistical mechanical model of diffusion of complex penetrants in polymers. *J. Polym. Sci., Polym. Phys. Ed.,* 17:1675–1692.

Pope, J. M., L. W. Walker, and D. Dubro. 1984. On the ordering of *n*-alkane and *n*-alcohol solutes in phospholipid bilayer model membrane systems. *Chem. Phys. Lipids.* 35:259–277.

Rowlinson, J. S. 1970. Structure and properties of simple liquids and solutions: a review. *Faraday Discuss. Chem. Soc.* 49:30–42.

Rowlinson, J. S., and B. Widom. 1982. Molecular Theory of Capillarity. Clarendon Press, Oxford.

Rychaert, J. P., and A. Bellemans. 1975. Molecular dynamics of liquid *n*-butane near its boiling point. *Chem. Phys. Lett.* 30:123–125.

Salem, L. 1962. Attractive forces between long saturated chains at short distances. *J. Chem. Phys.* 37:2100–2113.

Scheutjens, J. M. H. M., and G. J. Fleer. 1979. Statistical theory of the adsorption of interacting chain molecules. 1. Partition function, segment density distribution, and adsorption isotherms. *J. Phys. Chem.* 83: 1619–1635.

Schnitzer, J. E. 1988. Analysis of steric partition behavior of molecules in membranes using statistical physics. Application to gel chromatography and electrophoresis. *Biophys. J.* 54:1065–1076.

Seelig, A., and J. Seelig. 1974. The dynamic structure of fatty acyl chains in a phospholipid bilayer measured by deuterium magnetic resonance. *Biochemistry.* 13:4839–4845.

Theodorou, D. N. 1988. Microscopic structure and thermodynamic properties of bulk copolymers and surface-active polymers at interfaces. 1. Theory. *Macromolecules.* 2:1411-1421.

Theodorou, D. N. 1989. Variable-density model of polymer melt/solid interfaces: structure, adhesion tension, and surface forces. *Macromolecules.* 22:4589–4597.

Viovy, J. L., W. M. Gelbart, and A. Ben-Shaul. 1987. Scaling properties of chain interactions in amphiphilic aggregates. *J. Chem. Phys.* 87: 4114–4125.

Warner, M. 1980. Interaction energies in nematogens. *J. Chem. Phys.* 73: 5874–5883.

White, S. H., and G. I. King. 1985. Molecular packing and area compressibility of lipid bilayers. *Proc. Natl. Acad. Sci. USA.* 82:6532–6536.

White, S. H., G. I. King, and J. E. Cain. 1981. Location of hexane in lipid bilayers determined by neutron diffraction. *Nature (Lond.).* 290:161–163.

Wiener, M. C., and S. H. White. 1992. Structure of a fluid dioleoylphosphatidylcholine bilayer determined by joint refinement of x-ray and neutron diffraction data. III. Complete structure. *Biophys. J.* 61:434–447.

Wise, S. A., W. J. Bonnett, F. R. Guenther, and W. E. May. 1981. A relationship between reversed-phase C_{18} liquid chromatographic retention and the shape of polycyclic aromatic hydrocarbons. *J. Chromatogr. Sci.* 19:457–464.

Wise, S. A., and W. E. May. 1983. Effect of C_{18} surface coverage on selectivity in reversed-phase liquid chromatography of polycyclic aromatic hydrocarbons. *Anal. Chem.* 55:1479–1485.

Xiang, T-X., F. Liu, and D. M. Grant. 1991. Stochastic dynamics of *n*-nonane and related molecules in solution compared with nuclear magnetic resonance coupled relaxation times. *J. Chem. Phys.* 95:7576–7590.

Xiang, T-X. 1993. A computer simulation of free volume distributions and related structural properties in a model lipid bilayer. *Biophys. J.* 65:1108–1120.

Xiang, T-X., X. Chen, and B. D. Anderson. 1992. Transport methods for probing the barrier domain of lipid bilayer membranes. *Biophys. J.* 62: 77–78.

Zheng, C., and G. Vanderkooi. 1992. Molecular origin of the internal dipole potential in lipid bilayers: calculation of the electrostatic potential. *Biophys. J.* 63:935–941.